

Investigation of a Class-F⁻¹ Power Amplifier with a Nonlinear Output Capacitor

Junghwan Moon, Seunghoon Jee, Jungjoon Kim, Junghwan Son, Seungchan Kim,
Juyeon Lee, Seokhyeon Kim, and Bumman Kim

*Department of Electrical Engineering and Division of Information Technology Convergence Engineering,
Pohang University of Science and Technology (POSTECH),
Gyeongbuk, 790-784, Republic of Korea, Tel: +82-54-279-5584, Fax: +82-54-279-8115
{jymoon, bmkim}@postech.ac.kr*

Abstract—The practical operating conditions of class-F⁻¹ amplifier are investigated by analyzing the current and voltage waveform shapings. The bifurcated current of the amplifier is generated by the saturated operation at the knee region, resulting in quasi-rectangular current. The voltage shaping is studied for the active device with linear and nonlinear output capacitors (C_{out} s). In the linear C_{out} case, the half-sinusoidal voltage can be formed only at deeply saturated region, in which the proper second harmonic current is generated. The second harmonic voltage can be built using a large second harmonic load. When the nonlinear C_{out} is included, the harmonic load-pull simulation results show that the half-sinusoidal voltage is formed by the second harmonic generation of C_{out} rather than by the second harmonic current. This waveform shaping process is quite different from that of the conventional class-F⁻¹ PA, and we call the amplifier with the nonlinear C_{out} as the saturated amplifier. This saturated amplifier delivers better power performance than that of the amplifier with linear C_{out} since the former one can better shape the current and voltage waveforms. In the experiment, the saturated amplifier is designed and implemented using Cree GaN HEMT CGH40010 at 2.655 GHz. It provides a power-added efficiency of 73.9% at saturated output power of 41 dBm.

Index Terms—Class-F⁻¹, efficiency, nonlinear capacitor, power amplifier (PA), saturated PA.

I. INTRODUCTION

Highly efficient power amplifiers (PAs) are an essential RF component for wireless communication systems to achieve small, reliable, and low cost transmitters [1]–[7]. For the efficient operation, several PA topologies, such as class-F, class-F⁻¹, and class-E, have been proposed and analyzed with respect to the current and voltage waveforms and optimum load impedances [1]–[7]. Unlike other topologies, information for design method and operational behavior of the class-F⁻¹ amplifier is scarce. In addition, most of the amplifiers are analyzed under assumption of a linear output capacitor (C_{out}) of a transistor, but the C_{out} is quite nonlinear.

In this paper, the waveform shaping process of the class-F⁻¹ amplifier is analyzed through the saturated operation at the knee region. A large out-of-phase second harmonic current, with respect to the fundamental current, can be generated by the saturated operation. Even for the linear C_{out} , this second harmonic current with a large second harmonic load can support the half-sinusoidal voltage waveform required for

the class-F⁻¹ amplifier. However, for the real device including the nonlinear C_{out} , the C_{out} is the real one to shape the voltage by generating the out-of-phase second harmonic voltage component. The saturated amplifier, taking advantage of the nonlinear C_{out} to shape the voltage waveform, delivers better power performance than that of the classical class-F⁻¹. In this amplifier, it prefers a large third harmonic impedance instead of the short impedance of the conventional class-F⁻¹ PA. The implemented amplifier using Cree GaN HEMT CGH40010 at 2.655 GHz delivers the expected performance.

II. ANALYSIS FOR OPERATION CHARACTERISTICS OF CLASS-F⁻¹ AMPLIFIER

A. Class-F⁻¹ Amplifier with Linear Output Capacitor

The class-F⁻¹ amplifier has a half-sinusoidal voltage waveform and a rectangular current shape to minimize the internal power dissipation for an efficiency of 100%. Ideally, these waveforms are achieved by the short-circuit at odd harmonics and the open-circuit at even harmonics [1]–[4]. In practical implementation at or beyond microwave frequency region, only a few harmonic terminations, up to 3rd harmonic, can be tuned due to the large C_{out} . This C_{out} may provide the short-circuits at the higher harmonic frequencies. The active device acts as a voltage controlled current source and the voltage waveform generated by the load R_n is expressed as

$$\begin{aligned} V(\theta) &= V_{DC} - \sum_{n=1}^2 V_n \cdot \cos(n\theta + \varphi_n) \\ &= V_{DC} - \sum_{n=1}^2 I_n \cdot R_n \cdot \cos(n\theta + \varphi_n). \end{aligned} \quad (1)$$

where φ_n is phase of the n^{th} harmonic current. To achieve the half-sinusoidal voltage waveform with resistive loads for the fundamental and second harmonic terminations, a phase relationship between I_1 and I_2 should be out-of-phase. However, under the normal sinusoidal excitation of the PA, the second harmonic current with the phase relation cannot be obtained.

There are two methods to realize the out-of-phase condition between I_1 and I_2 : input voltage shaping and saturated operation. The input shaping can be made by the nonlinear input

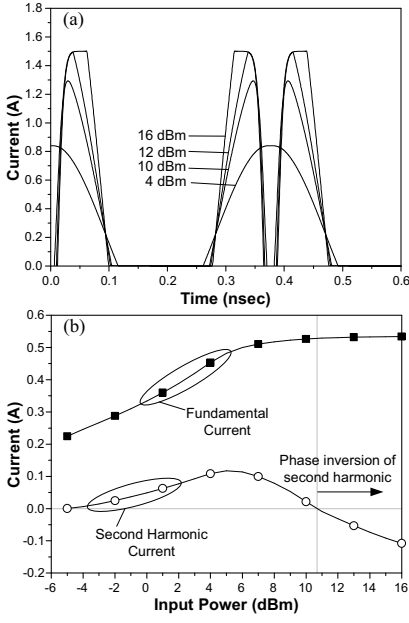


Fig. 1. (a) Output current waveforms according to the input power. The bifurcated currents are generated by the saturated operation at ohmic region. (b) The resulting fundamental and second harmonic currents. The current waveforms are calculated from ADS simulation with ideal transistor model, described in [7].

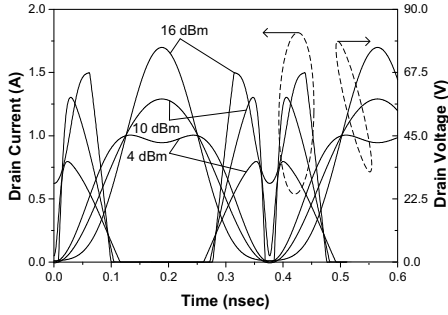


Fig. 2. Simulated time-domain voltage and current waveforms of the class-F⁻¹ amplifier with linear C_{out} .

capacitor, forming a quasi-rectangular output current with the proper phase relationship [1], [6]. In [7], however, we show that the input voltage shaping has a minor effect on the output voltage waveform when the nonlinear C_{out} is included. When PA is driven into deeply saturated region, the PA generates the bifurcated currents as shown in Fig. 1(a). For the input powers more than 11 dBm, as depicted in Fig. 1(b), the proper phase relationship between I_1 and I_2 is achieved. This means that the half-sinusoidal voltage for the class-F⁻¹ amplifier can be obtained by the highly saturated operation with purely resistive loads [4].

For proper operation of the class-F⁻¹ amplifier, the fundamental and second harmonic loads should be selected to maximize the fundamental voltage component. The amplifier can deliver the fundamental voltage $\sqrt{2}$ times larger than that of the tuned load (TL) amplifier when all harmonics except

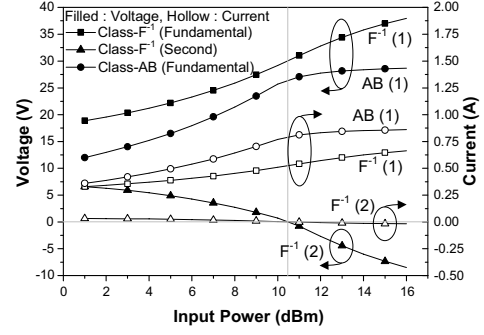


Fig. 3. Simulated voltage and current components of the class-F⁻¹ and class-AB amplifiers with linear C_{out} .

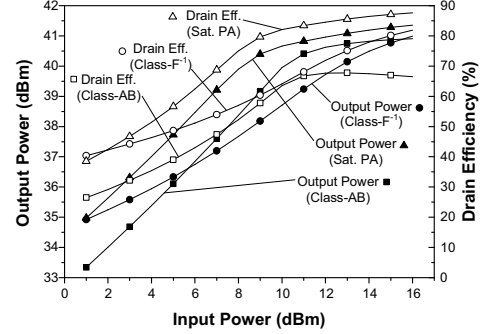


Fig. 4. Simulated output powers and drain efficiencies of the class-F⁻¹, class-AB, and saturated amplifiers. The saturated amplifier includes the nonlinear C_{out} , but the others have the linear C_{out} .

for the second harmonic component are shorted and V_2/V_1 in (1) is $\sqrt{2}/4$ [4], [7]. This increased voltage is generated by the load $\sqrt{2}$ times larger than that of TL amplifier. Such an enlarged load impedance leads the amplifier to the deeply saturated operation, lowering the fundamental current. Thus, assuming the same V_{DC} for both the class-F⁻¹ and the TL PAs, the fundamental load of class-F⁻¹ amplifier should be increased by more than $\sqrt{2}$ times larger than that of the TL amplifier.

Based on the presented theoretical analysis, the class-F⁻¹ PA is designed using the ideal active device model with linear C_{out} described in [7]. This model has a maximum current (I_{max}) of 1.5 A, a knee voltage of 4 V, and a constant g_m characteristic. For comparison, a TL PA is also designed. The PAs are biased at 14.8% I_{max} , a conduction angle of 200° , and have drain supply voltage of 30 V. For the TL PA, the fundamental load impedance is set to 33.35Ω . As mentioned, the fundamental load of the class-F⁻¹ should be larger than $47.16 \Omega (=33.35 \times \sqrt{2} \Omega)$ to deliver the large voltage swing. In this simulation, the fundamental load is set to 57.3Ω , which is found by sweeping the load to optimize the efficiency and output power, and the second harmonic is set to 300Ω . Fig. 2 shows the simulated time-domain voltage and current waveforms of the class-F⁻¹ and Fig. 3 represents the voltage and current components of the class-F⁻¹ and class-AB PAs. Due to the improper phase relation between I_1 and I_2 for

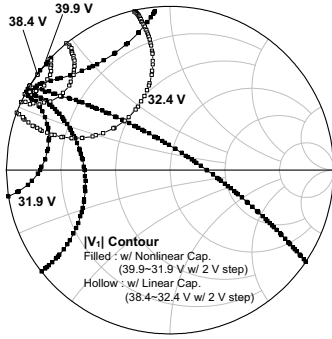


Fig. 5. Second harmonic load-pull result of the amplifiers with linear and nonlinear C_{out} s: $|V_1|$ contours at the input power of 16 dBm. The fundamental loads for the amplifiers are the same impedance level of 57.3Ω with the shorted higher harmonic loads.

the input power below 11 dBm, the voltage waveforms are different from those of the class- F^{-1} . However, as expected, the correct half-sinusoidal waveform is generated at the high input power levels above 11 dBm. Compared with the class-AB PA with the same drain bias, the class- F^{-1} has larger fundamental voltage and smaller fundamental current because of the larger load impedance. Thus, at the input more than 11 dBm, the efficiency of the class- F^{-1} is a lot higher than that of class-AB PA, as shown in Fig. 4.

B. Class- F^{-1} Amplifier with Nonlinear Output Capacitor

So far, C_{out} is assumed to be linear, but actually, it is a nonlinear element. The behavior of the nonlinear C_{out} has been investigated in [7]. It is shown that the capacitor generates a large out-of-phase second harmonic voltage component with small higher harmonics even though only the fundamental current flows through the capacitor. Thus, the resultant voltage waveform can be the half-sinusoidal shape except when the external second harmonic load is short-circuit or conjugate match of the C_{out} . Fig. 5 shows the second harmonic load-pull contour for $|V_1|$ of the amplifiers with the linear and nonlinear C_{out} s. Compared to the linear capacitor case, the amplifier with the nonlinear capacitor has larger fundamental voltage over broader region of the second harmonic load. This result indicates that the proper second harmonic voltage is generated by the nonlinear C_{out} rather than by the second harmonic current.

In short, to generate the current waveform similar to the ideal class- F^{-1} PA, it should be driven in to saturated region with a large fundamental load impedance. The voltage waveform is shaped by the nonlinear C_{out} . The behavior of this class- F^{-1} PA with the nonlinear C_{out} is quite different from the classical class- F^{-1} and we call it the saturated amplifier [7]. Fig. 6 shows the drain efficiency (DE) and output power contour with respect to the second harmonic loads. During the second-harmonic load-pull simulation, the fundamental load impedances for both amplifiers are set to 57.3Ω and the other harmonics are shorted. Compared to the linear C_{out} , the amplifier with the nonlinear capacitor delivers higher DE and output power over the broader region of the second harmonic

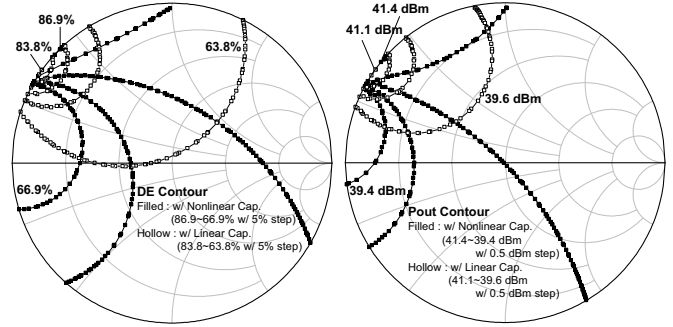


Fig. 6. Second harmonic load-pull results of the amplifiers with linear and nonlinear C_{out} s at the input power of 16 dBm: drain efficiency and output power contours.

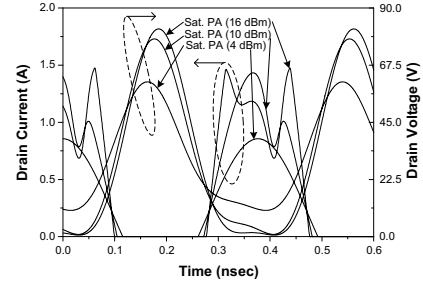


Fig. 7. Simulated time-domain voltage and current waveforms of the saturated amplifier.

load. This means that the second harmonic load has larger tolerance because the voltage waveform is mainly shaped by the nonlinear C_{out} . The maximum values of DE and output power are slightly increased because the nonlinear C_{out} generates not only harmonic voltages but also harmonic currents. The higher order harmonic currents are also generated by the saturated operation, enhancing the efficiency and output power. Fig. 7 shows the simulated time-domain voltage and current waveforms of the saturated amplifier. Compared to the class- F^{-1} with the linear C_{out} , the half-sinusoidal voltage waveform is maintained even at a low power region, indicating the harmonic generation at the region by the nonlinear C_{out} . Thus, the output power and efficiency are improved, as shown in Fig. 4. It is worth to note that, even though the third-harmonic impedance is shorted until now, the performances are further improved by tuning the impedance, usually a high impedance.

III. IMPLEMENTATION AND EXPERIMENTAL RESULTS

A saturated amplifier is designed and implemented at 2.655 GHz using a Cree GaN HEMT CGH40010 packaged device containing a CGH60015 bare chip. To investigate the inherent operational behavior of the saturated PA, the simulation is conducted using a bare-chip model. However, in the implementation, the packaged-device is employed. Fig. 8(a) shows the simulated second-harmonic load-pull contours for the output power and efficiency when the fundamental and third-harmonic impedances are set to $11.95 + j20 \Omega$ and

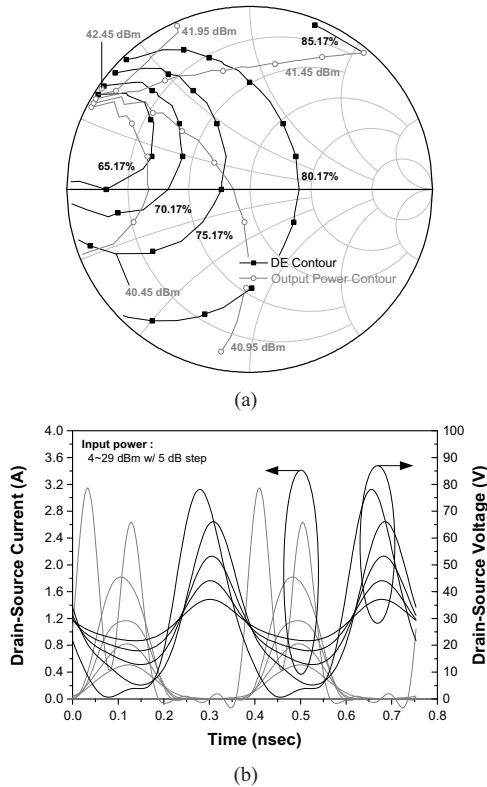


Fig. 8. Real device simulation results: (a) second harmonic load-pull contours for the output power and efficiency and (b) time-domain voltage and current waveforms of the saturated amplifier.

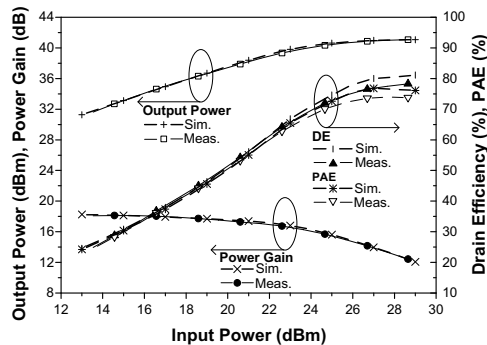


Fig. 9. Simulated and measured output power, drain efficiency, PAE, and power gain.

$0.7 - j31.7 \Omega$, respectively. Even though the third-harmonic impedance is short in Section II, the improved performance is obtained by loading a high third-harmonic impedance. As mentioned in Section II, the high efficiency and output power are maintained across broad second harmonic impedance level, proving that the nonlinear C_{out} shapes the voltage to the half-sinusoidal waveform. The second harmonic load for the maximum efficiency performance is $1.76 + j78.9 \Omega$. The simulated time-domain voltage waveforms in Fig. 8(b) show that the half-sinusoidal voltage waveforms are maintained even at the low power level, as well as at the high power level.

The designed PA is implemented on a RF35 substrate with $\epsilon_r = 3.5$ and thickness of 30 mil. In the experiment, the gate bias is set to -2.1 V ($I_{DSQ} = 210$ mA) at a supplied drain voltage of 28 V. The simulated and measured output power, efficiency, and gain characteristics for a CW signal are well matched, as shown in Fig. 9. In particular, the implemented PA provides a maximum PAE of 73.9% at a saturated output power of 41 dBm.

IV. CONCLUSIONS

The practical operating conditions of the class-F⁻¹ amplifier are analyzed with respect to the current and voltage waveform shapings. To form the half-sinusoidal voltage waveform with resistive loads, the phase relationship between the fundamental and second harmonic currents should be out-of-phase, which can be achieved by saturated operation. This saturated operation generates the bifurcated current. The fundamental load impedance should be larger than $\sqrt{2}R_{opt}$ because the half-sinusoidal voltage includes $\sqrt{2}$ times larger fundamental voltage than that of the TL PA. Under the condition, the amplifier can operate properly like a class-F⁻¹. However, in the practical case with the nonlinear C_{out} , the half-sinusoidal voltage is accomplished by the harmonic voltage generation of the capacitor. The operational behaviors of this amplifier are quite different from the conventional class-F⁻¹ amplifier, and we call it as a saturated amplifier. The saturated PA assisted by the nonlinear C_{out} for shaping the voltage and current waveforms is designed and implemented using a Cree GaN HEMT CGH40010 at 2.655 GHz. It provides a power-added efficiency of 73.9% and a saturated output power of 41 dBm.

ACKNOWLEDGEMENT

This work was supported by the MKE(The Ministry of Knowledge Economy), Korea, under the ITRC(Information Technology Research Center) support program supervised by the NIPA(National IT Industry Promotion Agency)(NIPA-2011-(C1090-1111-0011)) and WCU(World Class University) program funded by the Ministry of Education, Science and Technology through the National Research Foundation of Korea(R31-10100).

REFERENCES

- [1] S. C. Cripps, *RF Power Amplifiers for Wireless Communications*. 2nd ed. Norwood, MA: Artech House, 2006.
- [2] F. H. Raab, "Class-F power amplifiers with maximally flat waveforms," *IEEE Trans. Microw. Theory Tech.*, vol. 45, no. 11, pp. 2007–2012, Nov. 1997.
- [3] Y. Y. Woo, Y. Yang, and B. Kim, "Analysis and experiments for high-efficiency class-F and inverse class-F power amplifiers," *IEEE Trans. Microw. Theory Tech.*, vol. 54, no. 5, pp. 1969–1974, May 2006.
- [4] E. Cipriani, P. Colantonio, F. Giannini, and R. Giofrè, "Theoretical and experimental comparison of class F vs. class-F⁻¹ PAs," in *Proc. 40th Eur. Microw. Conf.*, Sep. 26–Oct. 1 2010, pp. 428–431.
- [5] N. O. Sokal and A. D. Sokal, "Class-E: A new class of high-efficiency tuned single-ended switching power amplifiers," *IEEE J. Solid-State Circuits*, vol. SC-10, pp. 168–176, Jun. 1975.
- [6] A. Grebennikov and N. O. Sokal, *Switchmode RF Power Amplifiers*. Burlington, MA: Elsevier, 2007.
- [7] J. Moon, J. Kim, and B. Kim, "Investigation of a class-J power amplifier with a nonlinear C_{out} for optimized operation," *IEEE Trans. Microw. Theory Tech.*, vol. 58, no. 11, pp. 2800–2811, Nov. 2010.